

Potential Antifibrotic Effect of Blueberry and Grape Polyphenol Extracts in Acute and Subacute Bleomycin-Induced Lung Tissue Injury Models in Mice

Potencial Efecto Antifibrótico de los Extractos de Polifenoles de Arándano y Uva en Modelos de Lesión Tisular Pulmonar Aguda y Subaguda Inducida por Bleomicina en Ratones

Zarina Shulgau¹; Yevgeny Kamyshanskiy¹; Shynggys Sergazy¹; Adilet Dautov¹;
Aigerim Zhulikeyeva¹; Alexandr Gulyayev¹ & Yerlan Ramankulov¹

SHULGAU, Z.; KAMYSHANSKIY, Y.; SERGAZY, S.; DAUTOV, A.; ZHULIKEYEVA, A.; GULYAYEV, A. & RAMANKULOV, Y. Potential antifibrotic effect of blueberry and grape polyphenol extracts in acute and subacute bleomycin-induced lung tissue injury models in mice. *Int. J. Morphol.*, 41(1):51-58, 2023.

SUMMARY: An experimental morphological and morphometric study of the antifibrotic function of blueberry and grape extracts was carried out on a model of lung injury in mice induced by intraperitoneal administration of bleomycin. During intraperitoneal administration of bleomycin to mice, acute and subacute damage to the pulmonary system was noted. Both patterns had the same prevalence and severity. The administration of polyphenolic extracts of blueberry and grape to mice showed a significant reduction in the severity of the acute and subacute pattern of lung injury. Blueberry and grape extracts reduce the acute phase of damage to the microvasculature, enhance phagocytic function, have an anti-inflammatory effect, reducing the degree of lymphohistiocytic infiltration and locoregional foci of residual inflammatory effects.

KEY WORDS: Fibrosis; Bleomycin; Polyphenols; Blueberry extract; Grape extract.

INTRODUCTION

It is generally accepted that pulmonary fibrosis is a very complex and fatal pathological process with limited possibilities of drug therapy (Huang & Tang, 2021; Moss *et al.*, 2022). Recent advances in finding the effects of individual polyphenols, e.g., resveratrol, curcumin, epigallocatechin, gallic acid, on the regulation of oxidative stress, inflammation, autophagy, and apoptosis suggest that damage minimization in pulmonary fibrosis is associated with the use of polyphenols (Bardelčíková *et al.*, 2022; Wang *et al.*, 2022; Zhongyin *et al.*, 2022). These results support the possibility of an antifibrotic effect when using biologically active compounds containing total polyphenols, in particular, it is possible to predict the likelihood of obtaining an antifibrotic effect when using polyphenolic extracts from blueberries or grapes.

MATERIAL AND METHOD

Grape extract. Cabernet Sauvignon – old French grape variety of medium-term maturity, currently located in Almaty and Zhambyl regions of Kazakhstan, were used in the study. The concentrate polyphenols obtained from seed ridges and grape skin – secondary wine products using water-alcohol feedstock extraction (40 % aqueous-alcoholic solution of ethyl alcohol in the ratio 1:5), followed by concentrating the extract on a rotary evaporator to a dry matter content of 25 %. The total concentration of phenolic derivatives in the concentrate of grape polyphenols used in this experiment is 5,000 mg/L.

Blueberry extract. Polyphenols were sourced from wild blueberry that were collected in summer-autumn period of 2018 in Surgut district of Khanty-Mansiysk County of

the Tyumen region of the Russia. The concentrate polyphenols obtained from berry skin using water-alcohol feedstock extraction (40 % aqueous-alcoholic solution of ethyl alcohol in the ratio 1:5), followed by concentrating the extract on a rotary evaporator to a dry matter content of 25 %. The final concentration of phenolic derivatives of berry is of 5,000 mg/L.

Concentration of polyphenols in samples determined using a commercially available kit “Polyphenols Folin-Ciocalteu” (ENOLOGY line by BioSystems. Spain) according to the manufacturing guidelines. Principle of the method: polyphenols in the sample react with Folin-Ciocalteu reagent in basic media. The increase of coloration is proportional to polyphenols concentration in the sample. Gallic acid solution (2000 mg/L) was used as a standard.

Animals. The study was approved by the Institutional Animal Care and Use Committee (IACUC) of the National center for biotechnology (decision 04/AP09260159 dated 8 September 2020). The reporting in this study is in accordance with guidelines published by the National Centre for the Replacement, Refinement and Reduction of Animals in Research (ARRIVE guidelines). All research work with laboratory animals was performed in accordance with generally accepted ethical standards for the treatment of animals based on standard operating procedures that comply with the rules adopted by the European Convention for the Protection of Vertebrate Animals Used for Research and Other Scientific Purposes.

Adult female outbred CD-1 mice 8–10 weeks of age, weighing 22 ± 2 g were used in experiments. These lines of rodents are bred in the animal facility of the National Center for Biotechnology, Nur-Sultan, Kazakhstan. The animals were housed in a room with a controlled temperature and a 12 h light-dark cycle with unlimited access to standard food (SSNIFF V1534-300, HTLab AG, Heideck, Germany) and drinking water ad libitum.

Two weeks before experiments, animals were randomly distributed in cages by ten mice per cage. The animals were used after a 14 day adaptation period. The animals were preserved in the same groups and same cages to reduce the stress. As required by the IACUC for survival experiments, moribund animals meeting the euthanasia criteria were euthanized using CO₂. The euthanized animals were counted as dead.

Experimental Designs. Mice (n=40) were randomly assigned to one of 4 groups of 10 mice in each study group.

Group I (Intact animals) received 0.1 ml of sterile saline

intraperitoneally (manipulation control), similar to BLM, twice a week for 4 weeks, total number of BLM injections - 8. Animals in group I received drinking water intragastrically daily (manipulation control) for 4 weeks (28 days).

Group II (Control) - received 0.5 mg BLM per mouse in 0.1 ml sterile saline intraperitoneally, twice a week, for 4 weeks, total number of BLM injections - 8. Animals in group II received drinking water as treatment (placebo) intragastrically daily for 4 weeks (28 days).

Group III (Blueberry extract) - received 0.5 mg BLM per mouse in 0.1 ml of sterile saline intraperitoneally, twice a week, for 4 weeks, a total of 8 injections of BLM. Animals in group III received blueberry extract as treatment intragastrically daily (0.2 ml per mouse) for 4 weeks (28 days).

Group IV (Grape extract) - received 0.5 mg BLM per mouse in 0.1 ml sterile saline intraperitoneally, twice a week, for 4 weeks, total number of BLM injections - 8. Animals in group IV received grape extract as treatment intragastrically daily (0.2 ml per mouse) for 4 weeks (28 days).

Euthanasia of laboratory animals was carried out 28 days after the start of the experiment by carbon dioxide overdose.

Histopathological examination. After the animals were removed from the experiment, lung tissue cutting (determination of the optimal localization, sample size, cut direction and number of cuts) was carried out in accordance with Ruehl-Fehlert *et al.* (2003).

To avoid collapse, the trachea was immediately ligated, and intact lungs were removed and immersed in 10 % neutral buffered formalin for 24 hours. Sections (3 μ m), including the main bronchi of each lobe, were stained with: (1) hematoxylin and eosin to assess overall morphology and inflammatory infiltrate; (2) Masson's trichrome to demonstrate fibrosis, identify collagen fibers and newly synthesized collagen; (3) Gomori silvering to detect reticulin fibers.

Hematoxylin and eosin staining was used to determine the overall morphological pattern of the lungs, the inflammatory pattern, and interstitial edema. For histological assessment of pulmonary fibrosis, Masson's trichrome stain was used to detect an increased amount of collagen (Titford, 2009). For histological evaluation of reticulin fibers, Gomori silvering was used in accordance

with the protocol (ab236473 Reticulum Stain Kit (Modified Gomori's), 2018). When stained with silver, reticulin fibers look like thin, dark fibrils, and abnormalities in the structure of reticulin can be detected, which occur, for example, in pulmonary fibrosis (Titford, 2009).

Tissue sections 5 µm thick were made on a Leica SM 2000R rotary microtome. Microscopy of preparations was carried out on a Zeiss AxioLab 4.0 microscope. AxioVision 7.2 for Windows was used to photograph the images.

Damage pattern criteria. The acute injury pattern is a histopathological pattern of lung injury in animals in an experimental study, which is a stress-induced (BLM) disorder of the histoarchitectonics of the respiratory regions with the development of acute interstitial injury (edema) and granulocytic infiltration.

The pattern of subacute damage is a histopathological pattern of damage to the lungs of animals in an experimental study, which is a type of damage with a predominance of immature collagen fibers without the formation of diffuse fibrotic fields and a disorder of the obvious histoarchitectonics of the respiratory compartment with lymphocytic infiltration.

Type I collagen (mature collagen) is the most common collagen, which is a structural component of connective tissue and the predominant component of the interstitial membrane, which forms the structural and mechanical basis (matrix) of bones, skin, tendons, cornea, blood vessel walls and other connective tissues (Karsdal *et al.*, 2016).

Type III collagen (immature collagen, reticulin) is the second most common collagen, expressed in early embryos and throughout embryogenesis, in adults it is the main component of the extracellular matrix, distributed in the wall of large blood vessels and reticular fibers of hematopoietic organs (Liu *et al.*, 1997).

Morphometric study. Histomorphometric evaluation of acute interstitial injury (edema) and cellular infiltrate (Fig. 2).

Morphometric analysis was carried out by two independent researchers without information about the animal's belonging to the group and the intervention. Edema was assessed in the perivascular and peribronchial space per 100 vessels: "0 points" - no edema, "1 point" - <10 % of vessels, "2 points" - 11-30 % of vessels, "3 points" - >31 % of vessels.

Quantification of active inflammatory cells (plasma cells, lymphocytes and polymorphonuclear granulocytes) was carried out over the entire section area. The calculation was carried out on 1000 cells: 0 points - cell infiltrate less than 1 %, active inflammation is absent; 1 point - less than 10 % of cells, microfocal infiltration, mild inflammation; 2 points - less than 30 % of cells, macrofocal, moderate degree of inflammation; 3 points - more than 30 % of cells, diffuse, severe inflammation.

Giant multinucleated cells - a quantitative assessment was carried out over the entire area of the histological section: 0 points - the absence of giant multinucleated cells, 1 point - up to 5 giant multinucleated cells, 2 points - 6-10 cells, 3 points - more than 10 giant multinucleated cells.

Active macrophages with intracytoplasmic inclusions (foam cells) - quantitative assessment was carried out over the entire area of the histological section: 0 points - no foam cells, 1 point - up to 5 cells, 2 points - 6-10 cells, 3 points - more than 10 foam cells.

Histomorphometric evaluation of collagen fibers. Histopathological analysis of collagen assessed its presence in the respiratory compartment (microvessels, alveoli, respiratory bronchioles), its distribution ("<5 %" - minimal, "6-30 %" - focal, ">30 %" - diffuse) and native structure ("discontinuous / continuous").

In histopathological analysis of reticulin fibers, the assessment was carried out in the central (perfusion) compartment (respiratory bronchioles, arteries and veins), and the peripheral (diffusion) respiratory compartment (microvessels, alveoli, respiratory bronchioles).

Histomorphometric evaluation of the reticulin fibers of the central compartment included an analysis of the structure of reticulin fibers: thin filamentous fibers with a clear margin or loose fibers with a blurred margin.

Histomorphometric assessment of reticulin fibers of the peripheral compartment included an analysis of the localization of reticulin fibers: localization is predominantly focal in the wall of thin alveolar septa or localization is predominantly diffuse in the wall of thickened alveolar septa.

For structural assessment of reticulin fibers of the peripheral respiratory compartment, the pattern of the native structure of reticulin fibers was assessed, including the structure of reticulin fibers and the distribution of reticulin fibers (uniform / chaotic).

Statistical Comparisons. Statistical data processing was

carried out using a spreadsheet Microsoft Excel (from the Microsoft Office 2010 package) and the software package for statistical analysis IBM SPSS Statistics 20.0. The Mann-Whitney test and c-square were used for pairwise comparison between the two groups. The Kruskal-Wallis test was used to compare several groups. Differences were considered significant if $p < 0.05$.

RESULTS AND DISCUSSION

We conducted an experimental morphological and morphometric study of the antifibrotic function of blueberry and grape extracts in a model of lung injury in mice induced by intraperitoneal administration of bleomycin.

Comparative histomorphometric characteristics data of interstitial edema and cellular infiltrate (hematoxylin and eosin stain) are presented in Table I.

In the intact group, the structure of the animal lungs in all cases corresponded to the histological norm.

In the control group, in 10 (100 %) cases, a pattern of severe acute interstitial injury was detected, of which: diffuse edema of the interalveolar septa (score 3, severe) in 7 (70 %) cases, moderate edema (score 2, moderate) was noted in 3(30 %) cases; macrofocal (score 2, moderate) and microfocal (score 1, mild) infiltration with polymorphonuclear granulocytes in 80 % and 20 % of cases, respectively; macrofocal (score 2, moderate) and diffuse (score 3, severe) infiltration with lymphocytes in 20 % and 80 % of cases, respectively; macrofocal (score 2, moderate degree) and microfocal (score 1, mild degree) infiltration by plasma cells in 60 % and 40 % of cases, respectively; diffuse (score 3, severe) infiltration by giant multinucleated

cells in 9 (90 %) cases. There were no cases with no infiltration by immune inflammatory cells.

In the group with blueberry and grape extracts, no severe acute interstitial damage was detected in all cases. The moderate histomorphometric pattern of edema in the group with blueberry extract was observed in 4 (40 %) cases and was of a microfocal nature. In the group with grape extract, moderate edema was observed in 1 (10 %) case, and mild interstitial edema was detected in 8 (80 %) cases.

Moderate chronic non-specific inflammation was noted in 5 (50 %) cases in the group with grape extract with moderate plasma infiltration. Mild chronic inactive inflammation was detected in 10 cases (100 %) in the blueberry extract group and in 4 (40 %) cases in the grape extract group. In all these cases, leukocyte infiltration was absent, in 1 (10 %) case in the group with blueberry extracts it was microfocal in nature (score 1, mild degree), and infiltration by plasma cells was microfocal (score 1, mild degree) or absent.

Giant multinucleated cells in the group with blueberry and grape extracts were observed in single histological sections in 10 % of cases. Single macrophages with cytoplasmic inclusions (foam cells) were detected in 20 cases (20 %) of animals in groups with blueberry and grape extracts.

The data of comparative histomorphometric characteristics of the pattern of subacute damage in the studied groups (staining with Masson's trichrome and Gomory's silver plating) are presented in Tables II and III.

In the intact group, no collagen fibers were found in the respiratory compartment, the distribution of available collagen is minimal (<5 %), the native structure is discontinuous, filamentous, and ordered.

Table I. Histomorphometric characteristics of interstitial edema and cellular infiltrate.

Name of indicator	Intact animals (n=10) (M±SD)	Control (n=10) (M±SD)	Blueberry extract (n=10) (M±SD)	Grape extract (n=10) (M±SD)
Edema *	-	2.70±0.48	0.40±0.52	1.00±0.47
Polymorphonuclear leukocytes**	-	1.80±0.42	0.10±0.32	-
Lymphocytes**	-	2.80±0.42	1.00±0.00	1.40±0.70
Plasma cells**	-	1.60±0.52	0.50±0.53	0.30±0.48
Multinucleated giant cells***	-	2.90±0.32	0.10±0.32	0.20±0.42
Macrophages with cytoplasmic inclusions (foam cells)***	-	-	2.80±0.42	2.50±0.53

*«0 points» - no edema, «1 point» <10 %, «2 points» 11-30 %, «3 points» >31 %

** «0 points» - less than 1 % cellular infiltrate, no active inflammation, «1 point» - less than 10 % of cells, microfocal infiltration, mild inflammation, «2 points» - less than 30 % cells, macrofocal, moderate inflammation, «3 points» - more than 30 % of cells, diffuse, severe inflammation.

*** «0» - absence of giant multinucleated cells/macrophages with cytoplasmic inclusions, «1» - up to 5 giant multinucleated cells/macrophages with cytoplasmic inclusions, «2» - 6-10 giant multinucleated cells/macrophages with cytoplasmic inclusions, «3» - more than 10 multinucleated giant cells/macrophages with cytoplasmic inclusions.

Table II. Histological and morphometric characteristics of collagen (profibrotic) fibers in the diffusion (respiratory) section of the lungs.

Name of indicator	Intact animals (n=10) (n/ %)	Control (n=10) (n/ %)	Blueberry extract (n=10) (n/ %)	Grape extract (n=10) (n/ %)
Respiratory compartment				
microvessels	-	10/100	10/100	10/100
alveoli, respiratory bronchioles	-	-	-	-
Distribution				
minimally (<5 %)	10/100	8/80	10/100	10/100
focally (<30 %)	-	2/20	-	-
diffusely (>30 %)	-	-	-	-
Native structure				
discontinuous	10/100	10/100	10/100	10/100
continuous	-	-	-	-
filamentous / ordered	10/100	10/100	10/100	10/100
macrofocal / chaotic	-	-	-	-

Table III. Morphometric assessment of the central (perfusion) and peripheral (diffusion) compartments of the lung.

Name of indicator	Intact animals (n=10)	Control (n=10)	Blueberry extract (n=10)	Grape extract (n=10)
Central (perfusion) compartment				
- Thin filamentous fibers with clear margin	10/100	10/100	10/100	10/100
- Loose fibers with blurred margin	-	-	-	-
Peripheral (respiratory) compartment				
- Thin filamentous fibers with clear margin	10/100	8/80	10/100	9/90
- Loose fibers with blurred margin	-	2/20	-	1/10
- Localization is predominantly focal in the wall of thin alveolar septa	10/100	8/80	10/100	9/90
- Localization is predominantly diffuse in the wall of thickened alveolar septa	-	2/20	-	1/10
- uniform distribution	10/100	8/80	9/90	9/90
- chaotic distribution	-	2/20	1/10	1/10

In the control group, all animals had single collagen fibers in microvessels and alveoli of the respiratory compartment; collagen fibers were minimally distributed in 8 (80 %) cases, and focally distributed in 2 (20 %) cases. The native structure of collagen is discontinuous, filamentous and ordered. In 2 (20 %) cases in the respiratory compartment, loose fibers with a blurred margin were observed, and in 2 (20 %) animals, diffuse fibers were observed in the wall of thickened alveolar septa, distributed chaotically.

In groups with blueberry and grape extracts, the histological pattern was characterized by the predominance of resorbable immature collagen fibers of type III (reticulin) in 90 % of cases, localized mainly focally in the wall of thin alveolar septa and evenly distributed, in 1 (10 %) case there were single fibers with blurred margins distributed randomly. Comparative histopathological evaluation of the pattern of bleomycin-induced lung injury in mice revealed that the study groups showed histopathological features of the model

of acute and subacute interstitial lung injury. Microphotographs of the lungs of mice of the studied groups are shown in Figure 1.

We found that in the lungs of control group mice there was a crossover pattern of injury: both an acute injury pattern and a subacute injury pattern. The pattern of acute damage was characterized by a disorder of the histoarchitectonics of the respiratory sections with the development of acute interstitial edema and granulocytic infiltration. In histopathological sections, multifocal lymphomacrophage vasculitis and bronchiolitis, diffuse edema of the interalveolar septa, multi-row lymphohistiocytic infiltrate in the perivascular and peribronchial zones with the formation of wide couplings with rows were determined. The pattern of subacute damage was characterized by damage with a predominance of immature collagen fibers without the formation of diffuse fibrotic fields and a disorder of the histoarchitectonics of the respiratory compartment with lymphocytic infiltration.

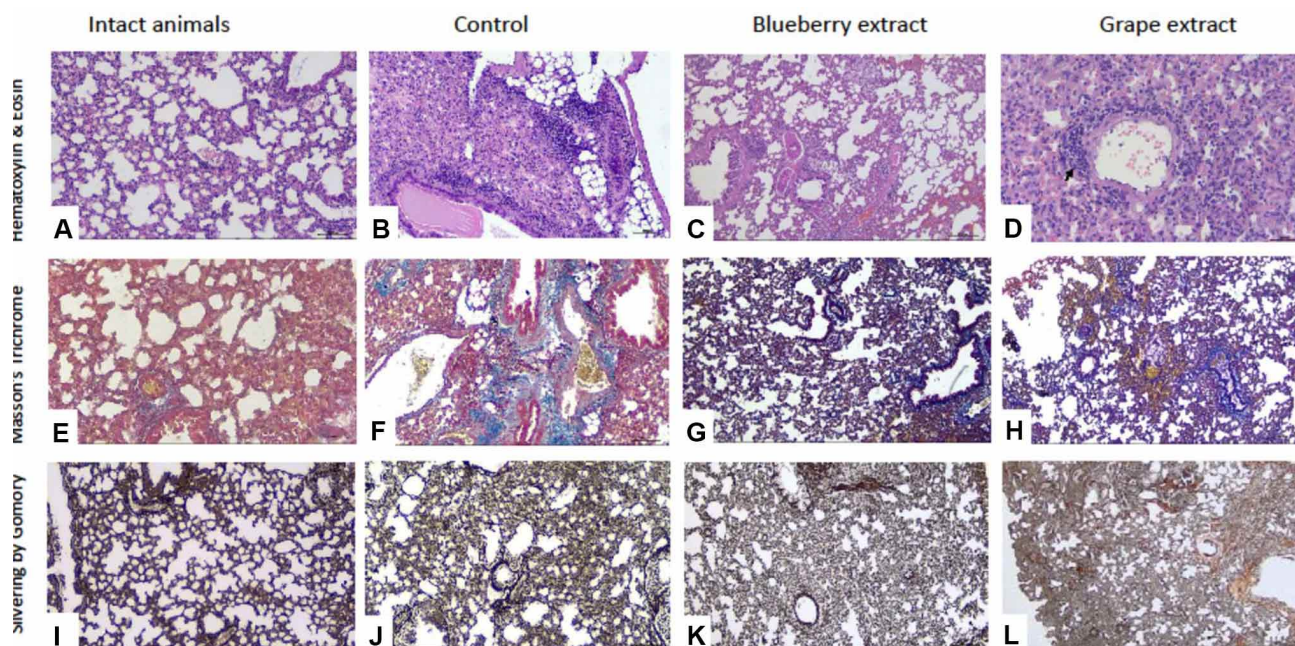


Fig. 1. Microphotographs of the lungs of mice. **A – Intact mice.** The morphological structure of the lung corresponds to the histological norm: thin interalveolar septa without signs of edema or inflammatory infiltration (hematoxylin and eosin stain, $\times 100$); **B – Control.** Multifocal lymphomacrophage vasculitis and bronchiolitis, diffuse edema of the interalveolar septa, multi-row lymphohistiocytic infiltrate in the perivascular and peribronchial zones with the formation of wide couplings with rows (hematoxylin and eosin stain, $\times 100$); **C – Blueberry extract.** Focal lymphomacrophage vasculitis and bronchiolitis, lymphohistiocytic infiltrate in the perivascular and peribronchial zones with the formation of couplings with rows (hematoxylin and eosin stain, $\times 100$); **D – Grape extract.** Focal lymphohistiocytic infiltrate in the interalveolar septa (hematoxylin and eosin stain, $\times 100$); **E – Intact mice.** Single peripheral short filamentous filaments of collagen fibers located in the respiratory compartment and collagen fibers in the wall of large vessels (Masson's trichrome stain, $\times 100$); **F – Control.** Filamentous collagen fibers located mainly in the region of the bronchiolo-alveolar junction (Masson's trichrome stain, $\times 200$); **G – Blueberry extract.** Single peripheral short filamentous filaments of collagen fibers (Masson's trichrome stain, $\times 200$); **H – Grape extract.** Single peripheral short filamentous filaments of collagen fibers (Masson's trichrome stain, $\times 200$); **I – Intact mice.** Thin filamentous structures diffusely distributed in alveoli and respiratory bronchioles; **J – Control.** Uniform distribution of reticulin fibers, but with a diffuse character and discontinuity in intra-alveolar and intravascular spaces. Reticulin fibers are characterized by a discontinuous arrangement with uneven fiber thickness, multiple areas of defibrillation on microfibers that extend into the perivascular space; **K – Blueberry extract.** Uniform distribution of reticulin fibers; **L – Grape extract.** Uniform distribution of reticulin fibers, but with a diffuse character and discontinuity in intra-alveolar and intravascular spaces.

Histochemical staining with Masson's trichrome revealed single peripheral short filamentous filaments of collagen fibers in the control groups. When using blueberry and grape extracts, collagen fibers in the periphery and in the central part were not detected, in the stromal component of the peripheral respiratory tissue, histochemical signs of profibrous collagen synthesis were not detected, in contrast to the control group ($p < 0.05$). The interstitial component of the respiratory zone of the lungs in the groups with blueberry and grape extracts is represented by a thin-fiber continuous connective tissue component with a fiber thickness that does not statistically significantly differ from the intact group.

In the histochemical study for reticulin in the control group, the lung parenchyma was lighter in tone of staining of reticulin fibers, in contrast to the group of intact

mice and groups with blueberry and grape extracts. Reticulin fibers were evenly distributed, but with a diffuse character and discontinuity in the intra-alveolar and intravascular spaces. Reticulin fibers are characterized by discontinuous arrangement with uneven fiber thickness, multiple areas of defibrillation on microfibers extending into the perivascular space and with a tendency to bulge into the lumen of the vessels. In the groups with blueberry and grape extracts, reticulin fibers were mainly represented by thin filamentous fibers with a clear margin, localized mainly in the wall of thin alveolar septa and evenly distributed, not statistically significantly different from the intact group ($p > 0.05$).

Lymphohistiocytic inflammatory infiltrate was predominantly noted in the peripheral zones, that is, in the respiratory zones of the lung tissue. When using blueberry

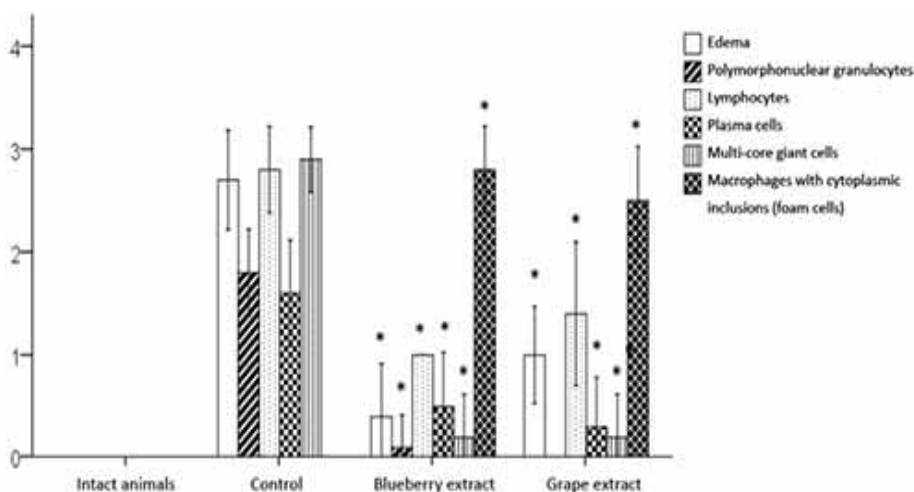


Fig. 2. Histomorphometric characteristics of the inflammatory pattern and interstitial edema.

and grape extracts, the lymphohistiocytic infiltrate was microfocal in nature with the formation of one to three rows with moderate lymphohistiocytic infiltration, with a statistically significant difference from the control group ($p < 0.05$), the interalveolar septa were thin, without visual signs of edema. Lymphohistiocytic infiltration was characterized by the formation of 1 to 3-layer cells of the couplings around the vessels and bronchioles.

In this study, the pattern of lung damage has a crossover nature of prolonged, constantly progressive damage, in which the damage patterns do not pass one into another, but there is a crossover. Previous studies have shown that bleomycin causes damage to the lungs, leads to hypoxia, reactive inflammatory processes and fibrotic processes, damage to the microvasculature of the respiratory system. More than one of these patterns may be present at the same time in each case (Isabela *et al.*, 2006; Hay *et al.*, 1987).

We have shown that blueberry and grape extracts cause improvement by acting on the microcirculatory bed, enhancing phagocytic function, reducing lymphohistiocytic infiltrates, locoregional foci of residual distant inflammatory effects, and reducing the acute phase of microcirculatory bed damage.

Blueberry and grape extracts contribute to the preservation of the structural histoarchitectonics of the lungs, which is manifested by the absence of severe acute inflammatory damage and a subacute pattern. The detected microfocal lymphomacrophage infiltration in the blueberry and kainar groups is nonspecific. Previously presented studies have shown that proliferation of lymphocytes in the lungs may be a non-specific sign of distant

consequences in the pathogenesis of bleomycin-induced pneumonitis (Seitzman *et al.*, 1998; Elewa *et al.*, 2021).

We also found that at the time of the study, there were no active processes in the lungs of mice, immune cells were chaotic, with a monotonous lymphohistiocytic infiltrate, located microfocally. These histopathological signs may be a non-specific sign of distant effects, however, these lymphohistiocytic infiltrates may also be a trigger mechanism for a locoregional focus of hypersensitivity during subsequent administration of the drug and cause uncontrolled progressive lung damage.

CONCLUSION

An experimental morphological and morphometric study of the antifibrotic function of blueberry and grape extracts was carried out on a model of lung injury in mice induced by intraperitoneal administration of bleomycin. During intraperitoneal administration of bleomycin to mice, acute and subacute damage to the pulmonary system was noted. Both patterns had the same prevalence and severity. The administration of polyphenolic extracts of blueberry and grape to mice showed a significant reduction in the severity of the acute and subacute pattern of lung injury. Blueberry and grape extracts reduce the acute phase of damage to the microvasculature, enhance phagocytic function, have an anti-inflammatory effect, reducing the degree of lymphohistiocytic infiltration and locoregional foci of residual inflammatory effects.

ACKNOWLEDGMENTS

The results of the research presented in the article were carried out within the framework of the grant "Search among bio- and synthetic antioxidants for new biologically active substances capable of inhibiting the development of pulmonary fibrosis" (Grant No. AP09260159), funded by the Science Committee of the Ministry of Education and Science of the Republic of Kazakhstan.

SHULGAU, Z.; KAMYSHANSKIY, Y.; SERGAZY, S.; DAUTOV, A.; ZHULIKEYEVA, A.; GULYAYEV, A. & RAMANKULOV, Y. El potencial efecto antifibrótico de los extractos de polifenoles de arándano y uva en modelos de lesión tisular pulmonar aguda y subaguda inducida por bleomicina en ratones. *Int. J. Morphol.*, 41(1):51-58, 2023.

RESUMEN: Se realizó un estudio experimental morfológico y morfométrico de la función antifibrótica de extractos de arándano y uva en un modelo de lesión pulmonar en ratones inducida por la administración intraperitoneal de bleomicina. Durante la administración intraperitoneal de bleomicina a ratones, se observaron daños agudos y subagudos en el sistema pulmonar. Ambos patrones tuvieron la misma prevalencia y severidad. La administración de extractos polifenólicos de arándano y uva a ratones mostró una reducción significativa en la severidad del patrón agudo y subagudo de lesión pulmonar. Los extractos de arándano y uva reducen la fase aguda del daño a la microvasculatura, mejoran la función fagocítica, tienen un efecto antiinflamatorio, reducen el grado de infiltración linfocítica y los focos localregionales de efectos inflamatorios residuales.

PALABRAS CLAVE: Fibrosis; Bleomicina; Polifenoles; Extracto de arándano; Extracto de uva.

REFERENCES

- ab236473 Reticulum Stain Kit (Modified Gomori's). Abcam, 2018. Available from: [https://www.abcam.com/ps/products/236/ab236473/documents/ab236473 %20- %20Reticulum %20Stain %20Kit %20\(Modified %20Gomori's\) %20v1a %20\(website\).pdf](https://www.abcam.com/ps/products/236/ab236473/documents/ab236473%20-%20Reticulum%20Stain%20Kit%20(Modified%20Gomori's)%20v1a%20(website).pdf)
- Bardelciová, A.; Mirossay, A.; Soltys, J. & Mojzis, J. Therapeutic and prophylactic effect of flavonoids in post -covid-19 therapy. *Phytother. Res.*, 36(5):2042-60, 2022.
- Elewa, Y.; Ichii, O.; Nakamura, T. & Kon, Y. Dual effect of bleomycin on histopathological features of lungs and mediastinal fat-associated lymphoid clusters in an autoimmune disease mouse model. *Front. Immunol.*, 12:665100, 2021.
- Hay, J.; Haslam, P.; Dewar, A.; Addis, B.; Turner-Warwick M. & Laurent, G. Development of acute lung injury after the combination of intravenous bleomycin and exposure to hyperoxia in rats. *Thorax*, 42(5):374-82, 1987.
- Huang, W. & Tang, X. Virus infection induced pulmonary fibrosis. *J. Transl. Med.*, 19:496, 2021.
- Isabela, C.; Silva, S. & Müller, N. L. Drug-induced lung diseases: Most common reaction patterns and corresponding high-resolution CT manifestations. *Semin. Ultrasound CT MR*, 27(2):111-6, 2006.
- Karsdal, M.; Leeming, D.; Henriksen, K. & Bay-Jensen, A. C. *Biochemistry of Collagens Laminins and Elastin: Structure Function and Biomarkers*. London, Elsevier, 2016.
- Liu, X.; Wu, H.; Byrne, M.; Krane, S. & Jaenisch, R. Type III collagen is crucial for collagen I fibrillogenesis and for normal cardiovascular development. *Proc. Natl. Acad. Sci. U. S. A.*, 94(5):1852-56, 1997.
- Moss, B.; Ryter, S. & Rosas, I. Pathogenic mechanisms underlying idiopathic pulmonary fibrosis. *Annu. Rev. Pathol.*, 17:515-46, 2022.
- Ruehl-Fehlert, C.; Kittel, B.; Morawietz, G.; Deslex, P.; Keenan, C.; Mahrt, C.; Nolte, T.; Robinson, M.; Stuart, B.; Deschl, U.; *et al.* Revised guides for organ sampling and trimming in rats and mice--part 1. *Exp. Toxicol. Pathol.*, 55(2-3):91-106, 2003.

- Seitzman, G. D.; Sonstein, J.; Kim, S.; Choy, W. & Curtis, J. L. Lung lymphocytes proliferate minimally in the murine pulmonary immune response to intratracheal sheep erythrocytes. *Am. J. Respir. Cell Mol. Biol.*, 18(6):800-12, 1998.
- Titford, M. Progress in the development of microscopical techniques for diagnostic pathology. *J. Histotechnol.*, 32(1):9-19, 2009.
- Wang, L.; Zhu, T.; Feng, D.; Li, R. & Zhang, C. Polyphenols from Chinese Herbal Medicine: Molecular mechanisms and therapeutic targets in pulmonary fibrosis. *Am. J. Chin. Med.*, 50(4):1063-94, 2022.
- Zhongyin, Z.; Wei, W.; Juan, X. & Guohua, F. Epigallocatechin gallate relieved PM2.5-induced lung fibrosis by inhibiting oxidative damage and epithelial-mesenchymal transition through AKT/mTOR pathway. *Oxid. Med. Cell Longev.*, 2022:7291774, 2022.

Corresponding author:

Shynggys Sergazy
Kurgalzhynskoye road 13/5
Astana, 010000
KAZAKHSTAN

E-mail: shynggys.sergazy@nu.edu.kz